GRAIN BOUNDARY MODELING AND CHARACTERIZATION OF THIN-FILM SILICON SOLAR CELLS

A.B. Sproul, S.A. Edmiston, T. Puzzer, G. Heiser, S.R. Wenham, and M.A. Green
Centre for Photovoltaic Devices and Systems, University of New South Wales, Sydney, 2052, Australia

T.L. Young
Pacific Solar, 82 - 86 Bay Street, Botany, NSW, 2019, Australia

ABSTRACT

An analytical model is developed to describe recombination currents arising from recombination at grain boundaries (GBs) in the depletion region of a *p-n* junction solar cell. Grain boundaries are modeled as having a single energy level in the energy gap, and partial occupancy of these states gives rise to a charge on the GB. The analytical model is compared to a complete numerical simulation package (DESSIS) and found to be in good agreement. Additionally, cross sectional EBIC images of a multilayer device containing vertical GBs are presented. Results derived from an analytical model are compared qualitatively to the experimental data and found to give good agreement.

INTRODUCTION

The multilayer cell seeks to make use of thin polycrystalline layers deposited on low cost, foreign substrates [1]. For thin layers of the order of 10 μm thick with grain sizes of about 5 μm it is to be expected that recombination at GBs will be the major limit to device performance. The multilayer cell seeks to overcome the problem associated with collecting photogenerated current in such material by incorporating additional collecting junctions. However, this additional current generating capability comes at the price of greater sensitivity to GB recombination within the *pn* junction regions, placing limits on the voltage capability of the device. In this paper we present an analytical model which describes more accurately the recombination current arising from GB recombination within the junction depletion region.

ANALYTICAL MODEL

To model GBs we use the "neutral level" formulation which has been developed elsewhere [2]. If the Fermi energy is at the "neutral level", the charge on the GB is zero. As the Fermi energy increases, the charge on the GB becomes increasingly negative. For Fermi energies less than the neutral level the charge on the GB becomes positive. This models the observed behaviour of GBs in silicon. The energy levels at a GB are most accurately described as a continuum of energy states from the valence to the conduction band. However for simplicity only one energy state at mid-gap is used in the model with an effective density of trap states, with suitable capture cross sections.

In the bulk regions of a solar cell the charge on the GB induces a depletion region in the semiconductor volume adjacent to the grain boundary. This leads to enhanced recombination as the effective surface recombination velocity S_{eff} at the edge of the depletion region can be greater than the actual value of S_{GB} at the GB. The charge Q_{GB} also leads to enhanced recombination within the depletion region of a *pn* junction. For example a vertical GB will have an electric field associated with the GB charge, normal to the junction which is opposite to the electric field present in the junction region away from the GB. This reduced electric field leads to a higher recombination rate at the GB, within the depletion region, compared to the case where the electric field is assumed to be unaltered by the presence of a GB.

This reduction in the E field is calculated analytically from a knowledge of Q_{GB} and E_N, the peak value of the *pn* junction electric field well away from a GB. For our analytical model we calculate E_N using the depletion approximation for a *pn* junction with uniform and equal doping. Once the reduced electric field at the point of maximum recombination has been calculated from the above quantities, the contribution of each vertical grain boundary per unit length to the dark current density from the depletion region is given by [3]

$$J_{VGB} = q\pi\sqrt{S_n S_p}\, L_E n_i \sinh\left(\frac{qV}{2kT}\right), \qquad (1)$$

where $L_E = kT/qE$ and E is the peak value of the electric field normal to the *pn* junction at the point of maximum recombination. The other symbols have their usual

0-7803-3166-4/96/$5.00 © 1996 IEEE

meaning. A more detailed discussion of the model is given elsewhere [3,4].

Shown in Fig. 1 are the upper limits placed on the open circuit voltage V_{OC} taking into account only recombination at a vertical GB within the depletion region for a single junction device. The V_{OC} is plotted as a function of the trap state density and capture cross section of the grain boundary traps. Also shown are lines of constant grain boundary surface recombination velocity, S_{GB} (S_n= S_p). At low values of trap state density (less than 10^{12} cm^{-2}), device voltages are directly related to grain boundary surface recombination velocity. However, as the trap state density increases, the electrostatic effects discussed earlier enhance recombination, and make the device voltages more dependent upon trap state density. Device voltages above 600 mV are achievable with S_{GB} between 10^4 cm/s and 10^5 cm/s. However, it should be noted that these results are sensitive to grain size. A halving of the grain size will reduce device voltages by about 70 mV. Figure 1 also shows some isolated data points from the full numerical model (DESSIS [5]), which are in good agreement with the values determined analytically.

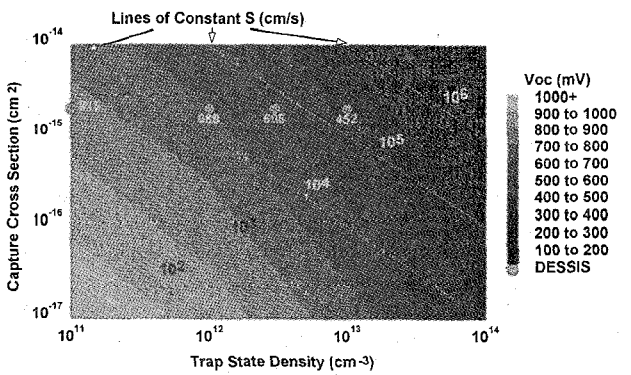

Fig. 1 : Open circuit voltage limits considering only recombination within a depletion region due to a vertical GB for a single *pn* junction. The doping of the layers is at 10^{18} cm^{-3} with an abrupt junction profile and the grain size is 5 μm.

By developing the analytical model presented here we have gained a better insight into the physics behind junction recombination at grain boundaries and now have a tool at our disposal which allows us to rapidly investigate the effect of GB recombination throughout a complete device. Such a tool will prove invaluable for optimising multilayer and conventional thin film, polycrystalline silicon solar cells.

EXPERIMENTAL

To characterize GB recombination in thin polycrystalline silicon multilayers we have made use of the Electron Beam Induced Current (EBIC) mode of the Scanning Electron Microscope. A test structure consisting of a 5-layer stack was grown on a polished multicrystalline silicon wafer (~ 1 Ω-cm, *p*-type) using CVD epitaxy (Lawrence Semiconductor Laboratories). The details of the layers are given in Table 1 (Further details of devices grown on CZ substrates are given elsewhere [6]).

The wafers were cut into 1 x 1 cm^2 pieces (using a Nd:YAG laser and cleaving through the multilayer stack), cleaned and oxidised (oxide thickness ~750Å). Doped grooves were then formed using a proprietary multilayer contacting process. The grooves were then metallized to allow electrical contact to be made to the parallel layers.

Layer #	Dopant type	Thickness (μm)	Concentration (cm^{-3})
1	n	0.8	1x10^{17}
2	p	2.8	1x10^{17}
3	n	2.2	1x10^{17}
4	p	6.4	1x10^{17}
5	n	4.8	1x10^{17}
Buffer layer	p	15	1x10^{18}

Table 1 : Details of CVD layers grown on a multicrystalline silicon substrate. The target thicknesses are reported. The actual thicknesses varied depending on the crystal orientation of individual grains. As and B were the dopant species.

RESULTS

Shown in Fig. 2 is a secondary electron image of the multilayer stack in the vicinity of a GB.

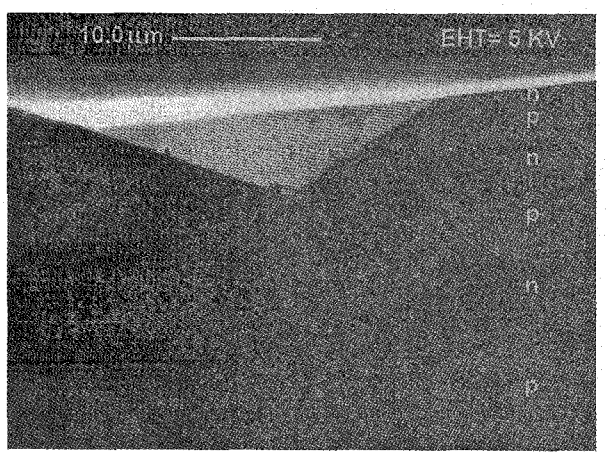

Fig. 2 : Cross section of the device. The image was obtained using secondary electron detection showing the various doped layers in the vicinity of a GB.

The banding that can be seen shows the location of the various *n* and *p* layers. We believe this contrast is due to slight differences in the oxide layer for *n* and *p* layers. The oxide was grown after cleaving of the sample. The V structure in the CVD film arises from the inhibition of the epitaxial growth at the GB which is located at the base of the V. Shown in Fig. 3 is an EBIC image of another region of the sample where the growth of the layer on either side of the GB was reasonably uniform. The top surface as well as the multilayer stack (edge on) are visible.

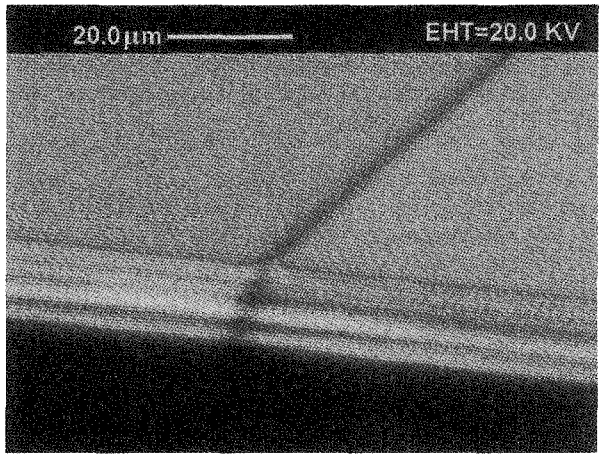

Fig. 3 : EBIC image (beam energy: 20 keV) of a GB passing almost vertically through a multilayer stack.

The GB is seen as the dark region where carriers are lost to recombination. Note that the cleaved edge clearly shows the good response of the 5 multilayers. The strongest response arises from where carriers are generated within the depletion regions of the adjacent layers. Away from the GB a decrease in the response occurs within the quasi-neutral regions of the layers. In part this is due to our present inability to effectively passivate the cleaved edge. Ultimately we aim to develop techniques that will passivate this cleaved surface such that the EBIC response is a measure of the minority carrier diffusion lengths within each layer. The underlying, heavily doped buffer layer, and substrate (dark region) produced no measurable EBIC current.

Of particular interest is the ability of this technique to image the recombination activity of the GB as it passes through the multilayer stack. A higher magnification EBIC image of the cross section is shown in Fig. 4 which shows greater detail of the GB region. Note the influence of GB recombination within quasi-neutral regions is limited to a relatively small volume by virtue of the multilayer design. Qualitatively these images are in good agreement with previously published modeled results [3].

Further analysis of the present data can be obtained by making use of a recent result which shows that the collection probability of photogenerated minority carriers is equal to a suitably normalised minority carrier concentration, for the device under dark, forward bias conditions [7] (for the 1D case). Other recent work has shown that this relationship holds in 2D as well [8], at least when uniformly doped as in this case. This greatly simplifies the modeling of GB effects as it is far easier to calculate the dark, minority carrier densities in the vicinity of a GB than it is to calculate analytically the collection probability. Making use of this result, shown in Fig. 5 is a plot of collection probability in a quasi-neutral *p*-layer in a multilayer stack, near a vertical GB.

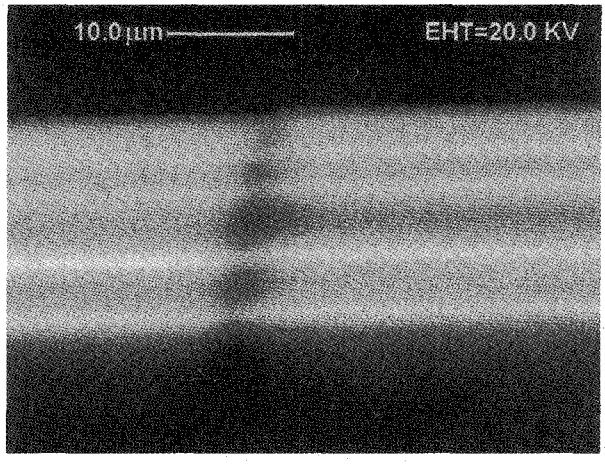

Fig. 4 : Higher magnification EBIC image (20 kV). The electron beam is incident at 90° to the cleaved surface.

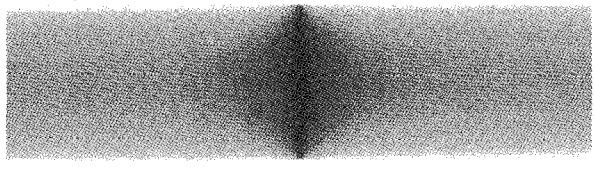

Fig. 5 : Calculated collection probability in the vicinity of a GB for a 20 µm wide by 5 µm thick *p*-layer, with L_n = 2.4 µm. A vertical GB is located at the centre of the layer. The darkest region corresponds to 0% while the lightest region corresponds to 100% collection probability.

The results were calculated using a 2D analytical, series-solution to describe the dark, minority carrier concentrations [9]. The following parameters were used in the calculations: S_{GB} = 10^7 cm/s, electron diffusion length L_n = 2.4 µm, and a dopant density 10^{18} cm^{-3}. The essential features of the modeled results agree well with the experimental EBIC images. The value of L_n corresponds to an effective value due to the effect of recombination at the cleaved surface. Note also that the collection probability calculated in Fig. 5 is the response of the layer to a point source excitation. However, for the EBIC image, the measured response would be modeled

by integrating the electron beam generation function [10] with the collection probability.

Shown in Fig. 6 is a similar EBIC image to Fig. 4 except now the accelerating voltage is 10 kV. This reduces the diameter of the generation volume D_G from about 4 μm for the 20 keV case to about 1 μm for the 10 kV case [10]. From Fig. 6 the EBIC image qualitatively approaches that represented by the modeled collection probability due to the increase in resolution at the lower accelerating voltage of 10 kV. Even higher resolution EBIC images have been obtained with beam energies of ~ 4 keV (D_G ~ 0.2 μm) but at present these images suffer from a low signal to noise ratio. However, with minor improvements to our present data acquisition system it should be possible to obtain high quality, sub-micron resolution EBIC images.

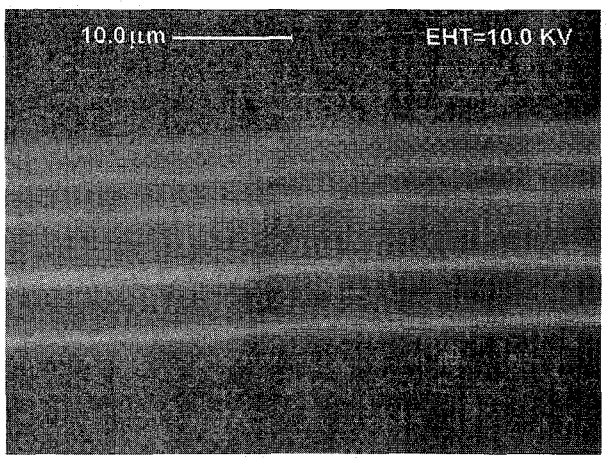

Fig. 6 : 10 kV EBIC image of the GB shown in Fig. 4.

CONCLUSIONS

The analytical model developed here to describe recombination at GBs within depletion regions is in good agreement with results obtained from a complete numerical simulation. The advantage of the analytical model is that it allows rapid calculations to be made which will be of benefit for optimising solar cell designs, particularly multilayer cells. Additionally we have shown that cross sectional EBIC imaging of multilayer structures is a valuable tool for investigating recombination properties of GBs. Good qualitative agreement with modeling has been achieved and future work is planned to quantitatively describe the data and extract parameters to fully describe GB recombination and diffusion lengths within layers.

ACKNOWLEDGMENTS

The authors gratefully acknowledge the contributions of Dr. M.R. Dickson and Dr. C. Martinic of the UNSW, Electron Microscope Unit and G.F. Zheng for assistance with device fabrication. This work was partly supported by Pacific Solar Pty. Ltd. The Centre for Photovoltaic Devices and Systems is supported by the Australian Research Council's Special Research Centres Scheme and by Pacific Power.

REFERENCES

[1] M.A. Green and S.R. Wenham, "Novel Parallel Multijunction Solar Cell", *Appl. Phys. Lett.* **65**, 1994, pp. 2907 - 2909.

[2] H.C. Card and E.S. Yang, "Electronic Properties at Grain Boundaries in Polycrystalline Semiconductors under Optical Illumination", *IEEE Trans. on Electron Dev.* **24**, 1977, pp. 397 - 402.

[3] M.A. Green, "Silicon Solar Cells : Advanced Principles and Practice", Centre for Photovoltaic Devices and Systems, Sydney , 1995.

[4] S.A. Edmiston, et. al., "Improved Numerical Modelling of Grain Boundary Recombination in Bulk and Junction Regions of Polycrystalline Silicon Solar Cells", to be published.

[5] "DESSIS 3.0 Manual", ISE Integrated Systems Engineering AG, Zurich, Switzerland, 1996.

[6] G.F. Zheng, et. al., "High-Efficiency CVD Multi-Layer Thin-Film Silicon Solar Cells", *Twenty Fifth IEEE PVSC*, 1996, to be published.

[7] T. Markvart, "Relationship Between Dark Carrier Distribution and Photogenerated Carrier Collection in Solar Cells", to be published, *IEEE Trans. on Electron Devices*, **43**, 1996.

[8] A.S. Al-Omar and M.Y. Ghannam "Direct Calculation Of Two-Dimensional Collection Probability in *pn* Junction Solar Cells, and Study of Grain-Boundary Recombination in Polycrystalline Silicon Cells", *J. Appl. Phys.* **79**, 1996, pp. 2103 - 2114.

[9] A.B. Sproul, et. al., "Innovative Structures for Thin Film Crystalline Silicon Solar cells to give High Efficiencies from Low Quality Silicon" *Twenty Fourth IEEE PVSC*, 1996, pp. 1563 - 1566.

[10] T.E. Everhart and P.H. Hoff, "Determination of Kilovolt Electron Energy Dissipation vs Penetration Distance in Solid Materials", *J. Appl. Phys.* **42**, 1971, pp. 5837 - 5846.